INVESTIGATING THE ENZYMOLOGY OF FE-S CLUSTER ASSEMBLY IN THE BACTERIAL ISC SYSTEM

A Thesis

by

HYERAN CHOI

Submitted to the Office of Graduate and Professional Studies of
Texas A&M University
in partial fulfillment of the requirements for the degree of

MASTER OF SCIENCE

Chair of Committee,	David P. Barondeau
Committee Members,	Marcetta Y. Darensbourg
	Coran M H. Watanabe
	Vishal M. Gohil
Head of Department,	Simon W. North

August 2016

Major Subject: Chemistry

ABSTRACT

Iron-sulfur (Fe-S) clusters are cofactors that are required for many biological processes. Conserved biosynthetic pathways synthesize Fe-S clusters and deliver clusters to target proteins using an elaborate distribution network. Both the cluster biosynthesis and transfer steps are tightly regulated to avoid the toxicity of labile iron and inorganic sulfide. The cysteine desulfurase, IscS, and the scaffold protein, IscU, constitute the core of the Fe-S assembly complex for the bacterial ISC pathway. IscS uses a pyridoxal 5'-phosphate cofactor to convert L-cysteine to L-alanine and mobilize sulfur as a persulfide intermediate for sulfur transfer to acceptor proteins. IscU combines this mobilized sulfur with ferrous iron and electrons to generate [2Fe-2S] clusters. [2Fe-2S]-IscU dissociates from IscS and participates in cluster transfer. Despite the importance of this pathway, the roles of additional protein components that interact with the assembly complex remain controversial, and mechanistic details for cluster synthesis and transfer are still poorly understood. Here, we take advantage of recently developed fluorescent reporter methodology to investigate the enzymology of the Fe-S cluster assembly reaction. A rhodamine fluorophore was used to label IscU and the decrease in fluorescence intensity (quenching) was used to monitor [2Fe-2S] cluster synthesis. The rate of [2Fe-2S]-IscU formation was determined as a function of each individual substrate (with the other substrates at high or saturating conditions) using a fluorescent plate reader located inside an anaerobic glovebox. Apo-IscU, an electron source (such as glutathione), ferrous iron, and L-cysteine were treated as substrates for the cluster assembly reaction. Some of the

substrates demonstrated a hyperbolic relationship between the rate of the reaction and the concentration of substrate, and kinetic parameters were determined by fitting the data to a Michaelis-Menten equation. Other substrates did not exhibit saturation behavior. A model consistent with these kinetic results is described that provides insight into this complex reaction and a base line for future studies interrogating the role of additional components, such as CyaY, IscX, Fdx, and IscA, proposed to have a role in the synthesis or regulation of Fe-S cluster formation.

DEDICATION

I would like to thank my undergraduate science professors and mentors who ignited my interest in science, and inspired and supported my pursuits. Without your guidance, I would never have come this far or felt the support that the scientific community has to offer its members.

Over the course of my life, I have been blessed with a loving and supportive family and loyal friends. This work is dedicated to each of them, for the specific roles they have played in my life and their never failing faith in me.

ACKNOWLEDGEMENTS

I would like to thank my advisor, Dr. David Barondeau, and my committee members, Dr. Marcetta Darensbourg, Dr. Coran Watanabe, Dr. Vishal Gohil, and Dr. Margaret Glasner, for their guidance and support throughout the course of this research.

I would also like to thank the Barondeau group members for their helpful insights and discussions during the course of this research. Thanks also go to my friends and colleagues and the department faculty and staff for making my time at Texas A&M University a great experience.

Finally, thanks to my mother and father for their encouragement and to my sister for her support and love.

TABLE OF CONTENTS

LIST OF FIGURES

LIST OF TABLES

CHAPTER I

INTRODUCTION

Iron-sulfur (Fe-S) clusters are protein cofactors that exhibit extremely versatile functions due to their diverse structural and redox properties. According to Wächtershäuser, Fe-S clusters may have played a vital role in the early anaerobic life on Earth and for that reason are often considered ancient cofactors [1]. Fe-S clusters are present in more than 500 enzymes or proteins and many of these are conserved in prokaryotic and eukaryotic organisms [2]. Nowadays, the unique biochemical properties of Fe-S proteins are readily used in various cellular processes such as respiration, electron transfer, gene regulation, catalysis, and DNA repair and replication [3, 4].

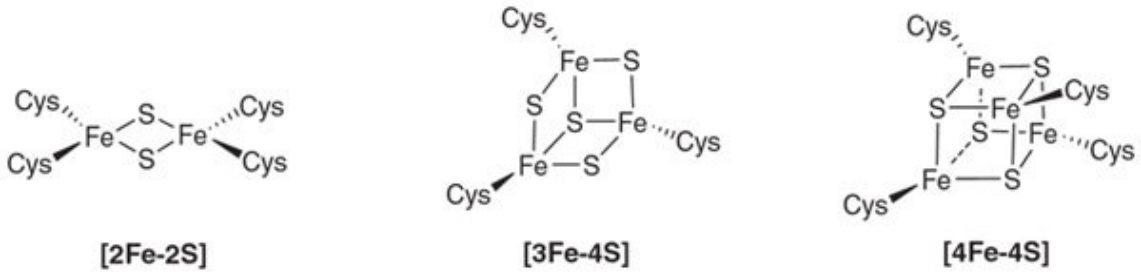

Figure 1-1. Structures of [2Fe-2S], [3Fe-4S], and [4Fe-4S] clusters. Reprinted with permission from *Nature Chemical Biology*, 2(4): 171-174. Copyright 2006 Nature Publishing Group.

Fe-S clusters can exist in various forms but the most common ones are the rhombic [2Fe-2S] cluster, [3Fe-4S] cluster, and cubic [4Fe-4S] clusters (Figure 1-1) [3]. They can

contribute to the protein function and also maintain structural integrity. More complex structures like the [8Fe-7S] cluster of nitrogenase in nitrogen fixing bacteria have been characterized. These clusters contain iron ($Fe^{2+/3+}$) and sulfide (S^{2-}) ion in a tetrahedral coordination and are typically ligated to the protein through cysteine residues. However, water or other amino acids such as histidine, arginine, lysine, serine, or aspartic acid can occasionally coordinate Fe-S clusters [4, 5]. This versatility gives rise to various functions for Fe-S clusters. Among their functions listed earlier, the most common feature would be the ability to deliver electrons. Since Fe-S clusters can delocalize electron density over Fe and S atoms and can exist in multiple redox states, they can act as both electron acceptors and donors in electron transfer [6-11]. The oxidation states vary between +2 and +3 valency and the redox potential ranges from -500 mV to +300 mV [3, 6, 7].

The basic building block for larger Fe-S clusters, the $[2Fe\text{-}2S]^{2+}$ cluster, is readily assembled *in vitro* with either ferric iron and sulfide, or in a more physiological reaction between ferrous iron, sulfane sulfur (S^0) derived from cysteine, and a reducing agent [12]. The sulfane sulfur, which is often in the form of a persulfide species, is reductively cleaved to generate sulfide during cluster synthesis. High levels of iron and sulfide are toxic to cells. Soluble Fe^{2+} readily shifts to the insoluble Fe^{3+} species in the presence of oxygen [13-15]. Ferrous iron also reacts with partially reduced oxygen species such as hydrogen peroxide through the Fenton reaction: $Fe^{2+} + H_2O_2 \rightarrow Fe^{3+} + {}^{-}OH + \bullet OH$. The produced free radicals react nonspecifically at nearly diffusion-limited rates with all biomolecules [16-19]. Sulfide in cells can also be harmful for various cellular processes such as oxidative phosphorylation by binding directly to heme iron [20]. In addition, Fe-S clusters

are vulnerable to reactive oxygen species (ROS) and oxidative stress induces cluster degradation. Overall, organisms highly regulate Fe-S cluster assembly in order to maintain physiologically tolerable levels and control the reactivity of free iron and sulfide.

There are three major Fe-S cluster assembly systems in bacteria and they are NIF (nitrogen fixation), ISC (iron-sulfur cluster), and SUF (sulfur mobilization) (Figure 1-2).

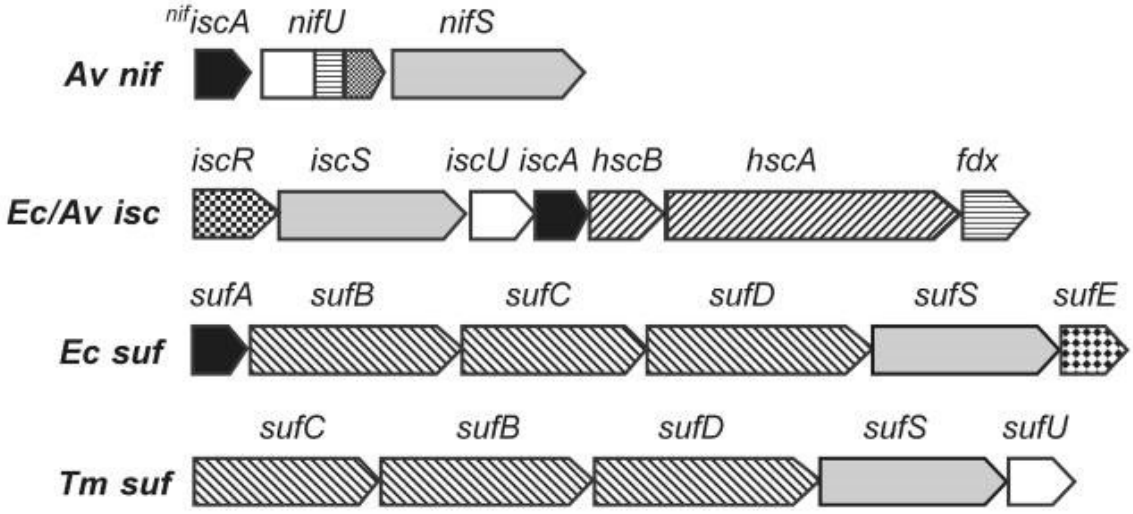

Figure 1-2. Genes in the NIF, ISC, and SUF systems of *Azotobacter vinelandii* (Av), *Escherichia coli* (Ec), and *Thermatoga maritima* (Tm). Adapted from Johnson *et al., Biochemical Society Transactions*, 2008 36: 1112-1119.

The NIF system was first discovered in *Azotobacter vinelandii*, and is essential to form the Fe-S clusters for nitrogenase and other proteins involved in nitrogen fixation [21-23]. Nitrogenase is found in diazotrophs that fix N_2 into ammonia. On the other hand, the ISC system provides Fe-S clusters for general "housekeeping" proteins [24]. The SUF

system is often specialized to activate under iron starvation or oxidative stress conditions [25].

The ISC system is encoded by the *iscRSUA-hscBA-fdx-IscX (isc)* gene cluster in *E. coli* [24]. This gene cluster encodes eight proteins. The first protein in the gene cluster is a [2Fe-2S] cluster containing protein, IscR, which is a transcriptional repressor that regulates the ISC gene cluster [26]. Interestingly, IscR binds [2Fe-2S] clusters and functions as a negative feedback control of Fe-S cluster synthesis. During oxidative stress or iron limiting conditions, apo-IscR is generated, which de-represses the ISC operon and leads to activation of the SUF system to stimulate Fe-S cluster production [27, 28]. Therefore, the IscR regulates the Fe-S clusters and prevents any excess Fe-S cluster generation.

After IscR, the ISC gene cluster encodes IscS, IscU, and IscA and they are involved in the basal Fe-S cluster assembly. IscS is a cysteine desulfurase that catalyzes conversion of L-cysteine into L-alanine and mobilizes sulfur for transfer reactions using a pyridoxal 5'-phosphate (PLP) cofactor [29]. Once the persulfide intermediate is generated by IscS, the sulfur is transferred to the scaffold protein, IscU. Early evidence showed that IscS and IscU form an $\alpha_2\beta_2$ hetero-tetrameric complex and suggested that the complex contains an inter-protein disulfide bond between Cys328 of IscS and conserved Cys63 of IscU [30]. IscU can act as a molecular platform for Fe-S cluster assembly. From the IscS protein-bound persulfide, iron atoms, and electron source, [2Fe-2S] cluster can be generated on IscU and transferred intact to apo-target proteins. IscA has been proposed to function in [4Fe-4S] cluster formation, as an iron donor, or as an alternate scaffold protein [31, 32].

HscB is a chaperone with ATPase activity, and HscA is a co-chaperone. HscBA complex stimulate the dissociation and/or transfer of Fe-S cluster from IscU to recipient proteins via a concerted sequence of protein interactions [33, 34]. Fdx, which contains a stable [2Fe-2S] cluster, is proposed to be the electron donor for the Fe-S biosynthesis [35, 36]. Also, Fdx may function in the reductive coupling of two [2Fe-2S] clusters to form a [4Fe-4S] cluster on IscU [37]. With NADPH and ferredoxin-$NADP^+$ reductase, Fdx has shown to provide electrons for Fe-S cluster assembly [38]. IscX interacts with both IscS and IscU [39], indicating that IscX may also be functioning as part of the Fe-S cluster assembly machinery. Although there is no direct evidence, IscX has been proposed to be an iron donor for cluster assembly due to its iron-binding properties [40].

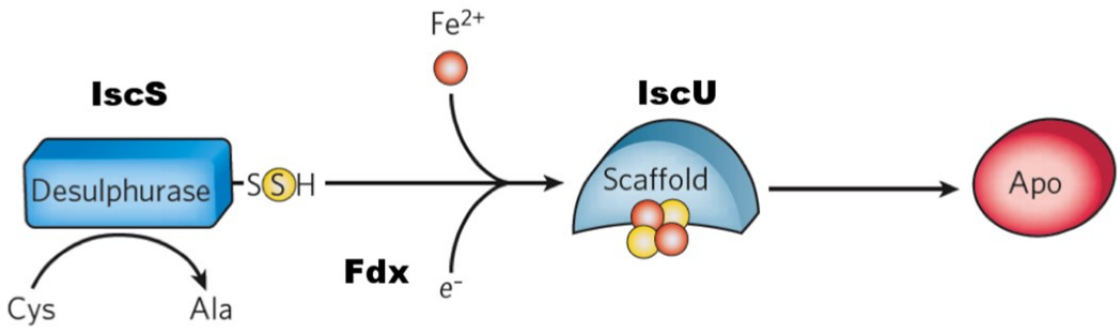

Figure 1-3. Fe-S cluster biosynthesis. A cysteine desulfurase enzyme catalyzes the PLP-dependent conversion of L-cysteine to L-alanine, and sulfur is combined with iron and electrons to build a Fe-S cluster on a scaffold protein. This intermediate cluster built on the scaffold protein will be transferred to an apo-protein target. Reprinted with permission from *Nature*, 460(7257): 831-838. Copyright 2009 Nature Publishing Group.

Fe-S cluster biosynthesis can be broken down into three major steps: 1) conversion of L-cysteine to L-alanine and sulfane sulfur production by a cysteine desulfurase; 2) *de novo* cluster assembly on a scaffold protein; and 3) transfer of the Fe-S cluster from the scaffold protein to apo-protein target (Figure 1-3). It is still unclear whether iron or sulfur is incorporated first in the assembly of Fe-S clusters on IscU. Both iron-first and sulfur-first models have been proposed (Figure 1-4) [41], but more investigation needs to be done to elucidate the mechanistic details of this pathway. In fact, these mechanisms presuppose a dimeric IscU species, which appears inconsistent with the known crystallographic structure of the IscU-IscS complex [42].

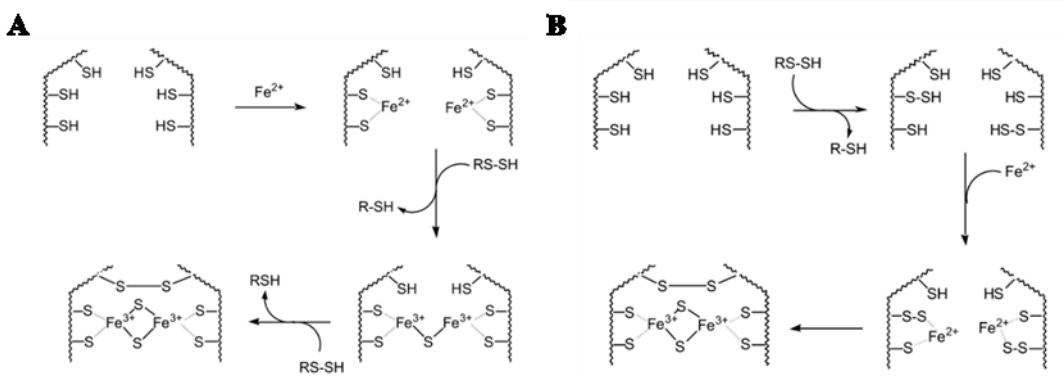

Figure 1-4. The two models, "Fe first, S second" (A) and "S first, Fe second" (B), for cluster assembly on the scaffold protein. Reprinted with permission from *Journal of Biological Inorganic Chemistry*, 10(7): 713-721. Copyright 2005 Springer Publishing Group.

The cysteine desulfurase provide sulfur to not only the ISC pathway but also to other proteins such as TusA, ThiI, and MoaD/MoeB [42]. Therefore, cysteine desulfurase's sulfur mobilization from L-cysteine is important for various biological

processes. In order to mobilize sulfur, the cysteine desulfurase first utilizes a PLP cofactor to form a Schiff base with the cysteine substrate (Figure 1-5). The aldamine intermediate delocalizes electrons into the PLP cofactor before carbon-sulfur cleavage through a nucleophilic attack by a mobile loop cysteine (Figure 1-6). The resulting persulfide intermediate on IscS can be cleaved to generate sulfide for measuring activity in enzymatic assays or the terminal sulfur can be transferred to cysteine residues on sulfur acceptor proteins in biosynthetic pathways. The controlling mechanisms for directing which sulfur acceptor protein (IscU, TusA, ThiI, and MoaD/MoeB) and ultimately which sulfur-containing biological pathway are poorly understood. Here in this thesis we aim to understand fundamentals of the enzymology for directing sulfur down the Fe-S assembly pathway.

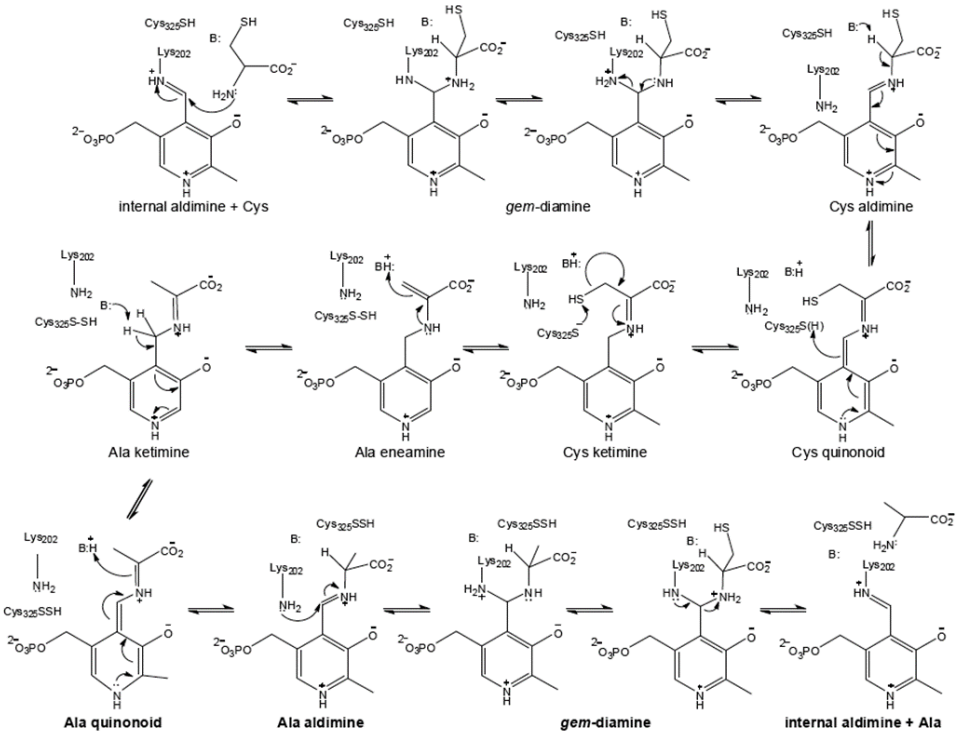

Figure 1-5. Mechanism of PLP catalyzed conversion of the L-cysteine to L-alanine with persulfide formation on the catalytic cysteine of the cysteine desulfurase. Adapted from Zheng *et al*., *Biochemistry*, 1994 33: 4714-4720.

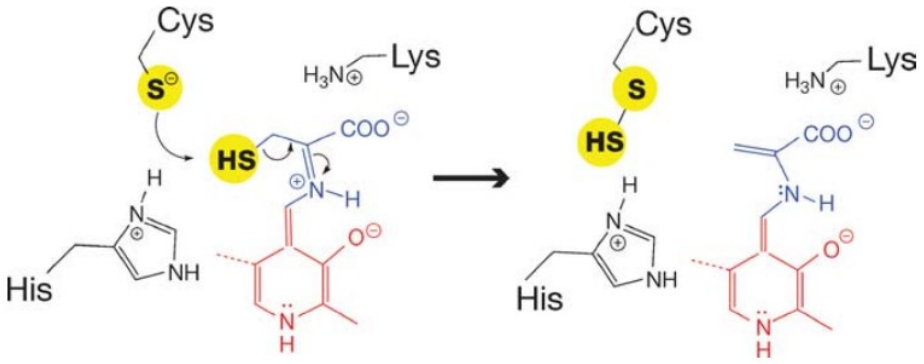

Figure 1-6. Cysteine desulfurase sulfur cleavage mechanism. An enzyme-bound persulfide is formed through the nucleophilic attack of the thiolate anion by the mobile cysteine loop. The substrate cysteine is shown in blue and the PLP is in red. Adapted from Johnson *et al*., *Annual Review of Biochemistry*, 2005 74: 247-281.

CHAPTER II

KINETIC CHARACTERIZATION OF THE BACTERIAL ISC SYSTEM

INTRODUCTION

The enzymology of Fe-S cluster biosynthesis is still poorly described despite the importance of this pathway. The substrate dependence and kinetic parameters for this reaction have not been well characterized and are important for evaluating the function of components such as IscA, IscX and CyaY. A challenge for performing these experiments is the limited sensitivity of the current assays, which use UV-Visible and circular dichroism spectroscopy to detect the cluster formation. We have recently developed a labeling strategy and a sensitive fluorescence-based assay that reports the Fe-S cluster content of labeled proteins [43]. This assay can be performed in parallel using a plate reader located inside an anaerobic glovebox.

The substrate dependence and kinetic parameters for the Fe-S cluster assembly reaction are currently poorly understood. Our objectives are to fluorescently label IscU with a rhodamine fluorophore ($IscU_{Rho}$) and monitor the development of [2Fe-2S]-$IscU_{Rho}$ using fluorescence quenching as a function of different substrates. The overall reaction can be written as:

$$Apo\text{–}IscU + 2\ e^- + 2\ Fe^{2+} + 2\ Cys \rightarrow [2Fe\text{–}2S]\text{–}IscU + 2\ Ala$$

The ISC biosynthetic machinery is centered on IscS, the cysteine desulfurase, which is the catalyst for mobilization of sulfur that is critical for the cluster formation reaction. Formally, the substrates for the reaction appear to be apo-IscU, reduced Fdx,

ferrous iron, and L-cysteine. First, the rate of holo-IscU formation will be measured with high concentrations of each substrate. Then, the concentrations of each substrate will be varied one at a time. With the use of fluorescence probe and/or circular dichroism (CD) spectroscopy, the rates of the reaction as a function of the different substrates (IscU, Fdx_{red}, Fe^{2+}, and Cys) will be measured. If there a hyperbolic relationship between the rate of the reactions and the concentration of substrate, then we will fit the rates to Michaelis-Menten's model and determine kinetic parameters such as K_m and V_{max}. However, if we do not observe Michaelis-Menten's kinetic like behavior, the substrate dependency can still be quantified with obtained rates and be compared with and without additional components such as CyaY, IscX, or IscA. From this study, one can gain more insights on mechanic details at the molecular level.

EXPERIMENTAL PROCEDURES

Protein Preparation. A plasmid with the IscS gene was transformed into BL21 (DE3) *E. coli* cells and the cells were grown at a temperature of 37 °C. Protein expression was then induced at an OD_{600} of 0.6 with 0.5 mM IPTG. The temperature was lowered to 16 °C, and cells were grown for about 16 hours. Through sonication (Branson sonifier 450), the cells were lysed in 50 mM HEPES pH 7.8, 250 mM NaCl (Buffer A) plus 5 mM imidazole and 100 μM PLP. After centrifugation of cells, the supernatant was loaded onto a 5 mL Ni-NTA column (GE Life Sciences) and was eluted with a linear gradient of Buffer A containing from 5 to 500 mM imidazole. Yellow fractions were collected, concentrated, and incubated with 10 mM DTT. The protein was further purified on a Sephacryl S300

column (26/60, GE Healthcare) that was previously equilibrated in 50 mM HEPES pH 8.0, and 250 mM NaCl.

Plasmid containing IscU gene was cloned into the NdeI and XhoI sites of pTwin1-His (Jena Bioscience) and was transformed into BL21 (DE3) *E. coli* cells. The cells were grown at a temperature of 37 °C. Protein expression was then induced with 0.2 mM IPTG when the OD_{600} was reached at 0.6. The temperature was decreased to 16 °C, and the cells were collected after about 16 hours. The cells were collected through centrifugation method and were lysed by sonication (Branson sonifier 450) in 50 mM NaH_2PO_4 pH 7.8, 250 mM NaCl (Buffer B), and 5 mM imidazole. The lysate was loaded onto a 5 mL Ni-NTA column (GE Life Sciences), and was eluded with a linear gradient of Buffer B that contained from 5 to 500 mM imidazole. The eluted protein from the Ni-NTA column was incubated with an equal volume of 400 mM Na_2S and 600 mM NaH_2PO_4 for 16 hours. Safety alert: 400 mM Na_2S and 600 mM NaH_2PO_4 need to be prepared in a fume hood by adding 1.2 M NaH_2PO4 to a solution of 800 mM Na_2S slowly. This incubation is for cleavage of intein linkage and for production of thiocarboxylate species. The incubated samples were dialyzed against a buffer of 50 mM NaH_2PO_4 pH 6.0, and 250 mM NaCl under a fume hood and reapplied to the Ni-NTA column. From the column, proteins were flowed through and collected to concentrate. After concentrated to about 1 mM, the samples were reacted with more than 5 equivalent of Lissamine-rhodamine B sulfonyl azide under the dark for 10 hours. The Lissamine-rhodamine B sulfonyl azide material was synthesized from sulforhodamine B acid chloride (Sigma-Aldrich) and sodium azide (Sigma-Aldrich) as previously described [44] and stored in DMSO at -20 °C. The

fluorescently labeled IscU sample was loaded onto a 1 mL anion column to remove excess fluorophore and also was washed well with 50 mM HEPES pH 7.8 buffer before elution. With gradual addition of up to 1 M NaCl to anion column, the pink samples were eluted from the anion column. The final sample was analyzed by SDS-PAGE and fluorescent gel imaging. The $IscU_{Rho}$ protein was successfully labeled with fluorophore and the excess unbound fluorophore had been removed. Protein concentration was determined through Bradford assay. Rhodamine B was quantitated from the extinction coefficient at 565 nm of 84,000 $M^{-1}cm^{-1}$ [45]. The purified $IscU_{Rho}$ was flash frozen in liquid nitrogen and stored in -80 °C.

Cysteine Desulfurase Activity Measurements. Reaction mixtures with a volume of 800 µL containing 0.5 µM IscS, 1.5 µM IscU, 2 mM DTT, 10 µM PLP, 5 µM $Fe(NH_4)_2(SO_4)_2$, 1.5 µM CyaY, 50 mM Tris pH 8.0, and 250 mM NaCl were incubated in an anaerobic glovebox (~12 °C) for about 30 minutes. The cysteine desulfurase reactions were initiated with the addition of 100 µM L-cysteine at 37 °C using a heat block and were quenched by addition of 100 µl of 20 mM *N,N*-dimethyl-*p*-phenylenediamine in 7.2 N HCl and 100 µl of 30 mM $FeCl_3$ in 1.2 N HCl. This step initiates the conversion of sulfide to methylene blue. After 20 minutes of incubation at 37 °C and centrifugation of 5 minutes at 12,000 rpm, the methylene blue formation was measured at 670 nm and then converted to sulfide production by using a Na_2S standard curve to quantification. The units for rate are µmol sulfide per µmol cysteine desulfurase per minute at 37 °C. The rates were fitted to the Michaelis-Menten equation by KaleidaGraph (Synergy Software).

Fluorescence Assays. Assays were performed using a Tecan M200 fluorescent plate reader with top-read fluorescence and bottom-read absorbance measurements. The fluorescent plate reader is located inside of an anaerobic glovebox with low oxygen level. For experiment, the greiner 96 well plates with black sides, clear flat bottoms, and a non-binding coating were used. Plates were pre-kept in the glovebox at least 10 hours before the use to make sure the oxygen that was previously dissolved in the plastic can diffuse out from the plates. The fluorescence of rhodamine labeled protein was measured with excitation wavelength of 550 nm and emission wavelength of 600 nm. Assays were monitored every 5 minutes for 2 hours at 25 °C and the plate was covered with low fluorescent clear tape on top during the measurements.

Fluorescence Data Processing. After the raw fluorescence data for the reaction ($F_{measured}$) was obtained, the raw data was corrected for the inner filter effect by using the absorbance of each well at the excitation (Abs_{ex}) and emission (Abs_{em}) wavelengths. Then, the fluorescence was corrected ($F_{reaction}$) using the Eq. 2-1.

$$F_{reaction} = F_{measured} \times 10^{\frac{(Abs_{ex}+Abs_{em})}{2}} - F_{auto} \times 10^{\frac{(Abs_{ex}+Abs_{em})}{2}}$$

(Eq. 2-1)

From the average fluorescent values from three wells containing only the buffer solution, F_{auto} was obtained and corrected for the inner filter effect with the equation 1. A reference sample (F_{ref}) was used to remove any fluorescence due to photobleaching or adhesion to the plate. For F_{ref}, the Eq. 2-2 was used from a control sample ($F_{control}$) which included the fluorescent protein ($IscU_{Rho}$) at the same concentration as the reaction but

missing a reagent that initiates the reaction. Inner filter effect and autofluorescence corrections was applied in the same manner as well.

$$F_{ref}=F_{control} \times 10^{\frac{(Abs_{ex}+Abs_{em})}{2}}-F_{auto} \times 10^{\frac{(Abs_{ex}+Abs_{em})}{2}}$$

(Eq. 2-2)

In the assay, the fluorescence intensity from the reference sample (F_{ref}) was scaled to be 100%. It was confirmed that the fluorescence signals from the sample and the reference wells at the initial time 0 were within error of each other. Then, the fluorescent signals were normalized by dividing the fluorescence at a time t by the fluorescence at a time 0 so that the fluorescence value starts from 1. Finally, the normalized fluorescence values of the reaction well and that of the reference well were divided to generate the final $(F_{reaction}/F_{ref})'_t$ value in Eq. 2-3.

$$\left(\frac{F_{reaction}}{F_{ref}}\right)'_t = \left(\frac{F_{reaction,\ t}}{F_{reaction,\ t=0}}\right) \Bigg/ \left(\frac{F_{ref,\ t}}{F_{ref,\ t=0}}\right)$$

(Eq. 2-3)

Fe-S Cluster Formation. Control quenching reactions included 30 μM $IscU_{Rho}$ in 50 mM HEPES pH 7.5, and 250 mM NaCl were performed for 2 hours at 25 °C. For the cluster assembly reaction of 100 μL, 0.5 μM IscS, 30 μM IscU, 400 μM $Fe(NH_4)_2(SO_4)_2$, 1 mM L-cysteine, and 10 mM GSH at pH 7.2 were used. The reaction was initiated by injecting L-cysteine at the end. The samples were mixed uniformly by pipetting up and down several times. Before placing the plate on the plate reader, the plate was covered with a low-fluorescent plastic tape. The temperature was kept at 25 °C during the

experiment. The fluorescence (excitation wavelength, 550 nm; emission wavelength, 600 nm) and absorbance (456, 550, and 600 nm) were measured every 5 minutes. In between measurements, the plate was shaken to minimize any localized photobleaching. The assay was monitored for 2 hours.

Michaelis-Menten Kinetics for Cluster Assembly. The rate of holo-IscU formation was measured with high concentrations of substrates which are apo-IscU, ferrous iron, L-cysteine, and GSH. The concentrations of each substrate was varied one at a time. After fluorescence data was processed, the initial linear quenching was fitted linearly to obtain the rates. The reaction rates were multiplied by the final holo-IscU concentration, which was determined from the final quenching value at the end of the reaction and assuming quenching value of 0.6 is equivalent to 100% quenching. The rate data were then plotted against the substrate concentration. Reactions that appeared to show saturation behavior were fit with the Michaelis-Menten equation in KaleidaGraph to obtain k_{cat} and K_M values. For reactions that did not show saturation behavior, the data were fitted to a linear equation to obtain the rate in $\mu M^{-1} \cdot min^{-1}$.

RESULTS

Michaelis-Menten Analysis of Fe^{2+} Dependence in Fe-S Assembly Reaction. First, ferrous iron was treated as a substrate, and its concentration was varied for the cluster assembly reaction in fluorescence quenching experiments. As the concentration of ferrous iron was increased from 0 to 400 μM, the quenching of the $IscU_{Rho}$ due to [2Fe-2S] cluster formation was recorded as a function of time (Figure 2-1). The fluorescence data was

processed to account for loss of fluorescence due to the inner filter effect, protein adsorption to the plates and photobleaching and plotted as a function of time. The apparent quenching rate was determined from the initial linear region and was multiplied with the concentrations of holo-$IscU_{Rho}$ formed at the end of the completion of the reactions. A change in initial rate of the reaction and extent of reaction (amount of [2Fe-2S]-IscU) was observed as the iron concentration was increased. Fitting this data to the Michaelis-Menten reaction equation (Figure 2-2) revealed an apparent k_{cat} of 0.36 ± 0.01 min^{-1} and K_M of 93 ± 11 μM.

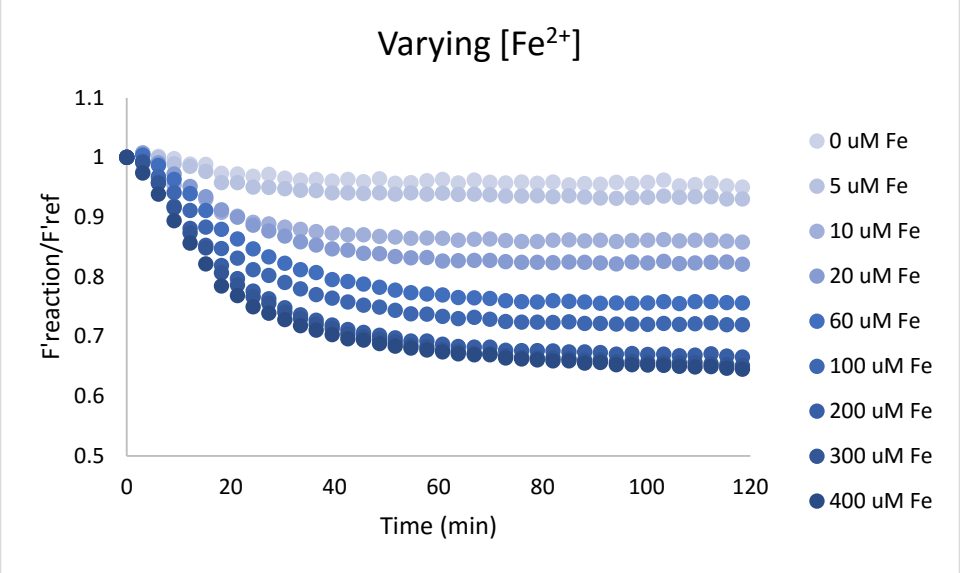

Figure 2-1. [2Fe-2S]-$IscU_{Rho}$ formation with various ferrous iron concentrations. Reactions contained IscS (0.5 μM), apo-$IscU_{Rho}$ (30 μM), L-cysteine (1 mM), glutathione (10 mM) and different concentrations of ferrous iron. Fe-S cluster formation was monitored by quenching of $IscU_{Rho}$ as a function of time.

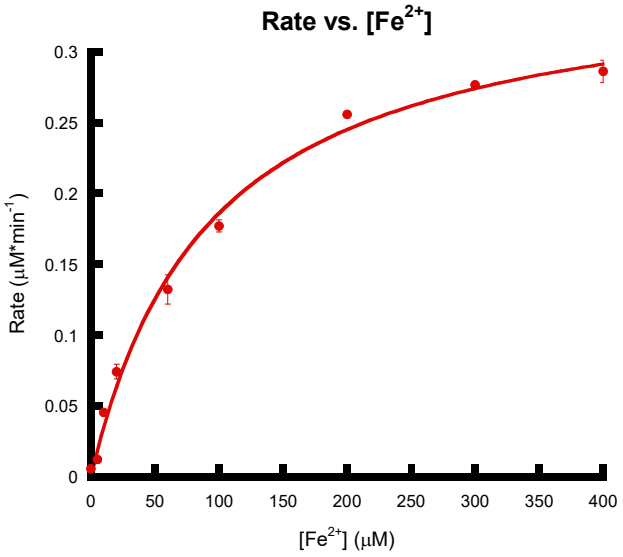

Figure 2-2. The rate of the reaction as a function of ferrous iron concentration. The plot was generated based on the data from Figure 2-1. The rates for each data points were obtained by multiplying the concentrations of holo-$IscU_{Rho}$ formed at the end of each reactions with rates from the initial linear regions of the quenching data.

Michaelis-Menten Analysis of Cysteine Dependence in Fe-S Assembly Reaction.

Cluster assembly rates were observed as the concentration of cysteine was increased. Here, the cysteine concentration was varied from 0 to 1.5 mM and fluorescence quenching experiment was performed (Figure 2-3). When the rate from the quenching data was plotted as a function of the cysteine concentration, a different trend from that obtained by varying the iron concentration result was observed. The relationship between the rate of the reaction and the cysteine concentration was found to be linear, and not a hyperbolic relationship (Figure 2-4). As the concentration of cysteine was increased, the rate of the reaction multiplied by the concentration of holo-$IscU_{Rho}$ assembled at the end of the reaction was also increased.

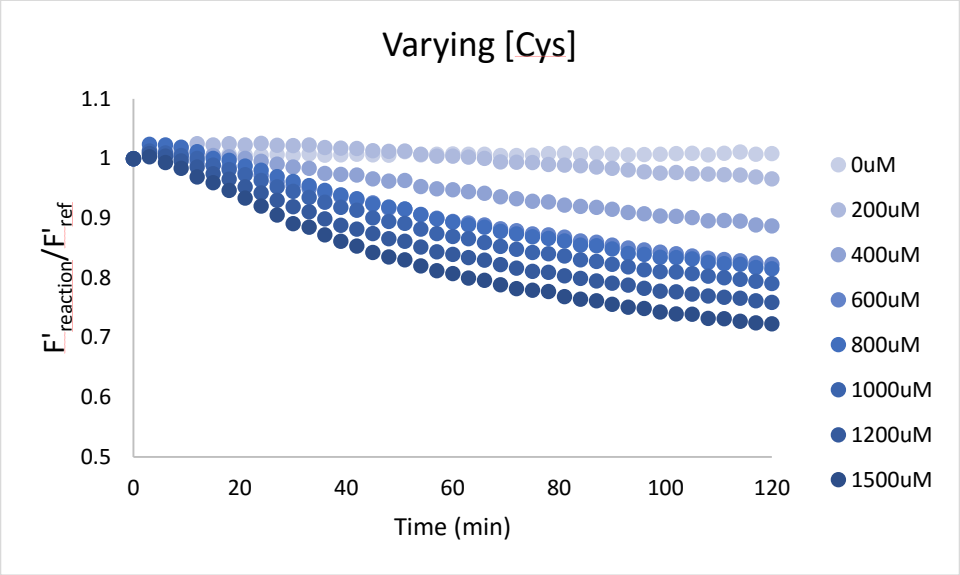

Figure 2-3. [2Fe-2S]-IscU$_{Rho}$ formation with various cysteine concentrations. Reactions contained IscS (0.5 μM), apo-IscU$_{Rho}$ (30 μM), ferrous iron (400 μM) and different concentrations of cysteine. Fe-S cluster formation was monitored by quenching of IscU$_{Rho}$ as a function of time.

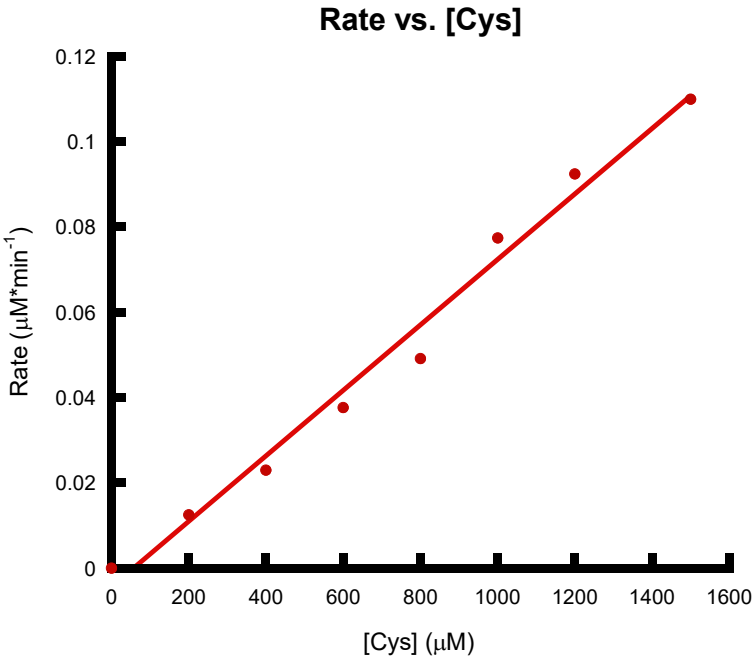

Figure 2-4. The rate of the reaction as a function of cysteine concentration. The plot was generated based on the data from Figure 2-3. The rates for each data points were obtained by multiplying the concentrations of holo-IscU$_{Rho}$ formed at the end of each reactions with rates from the initial linear regions of the quenching data.

Next, we repeated these experiments in the presence of glutathione (GSH). The cysteine concentration was varied from 0 to 2 mM for the cluster biosynthesis reaction, and each reaction now contained 10 mM GSH (Figure 2-5). When the rate of the reaction was plotted as a function of cysteine concentration, the graph displayed a different curve from the one did not contain GSH. Here, the graph did not fit well with neither linear trend nor Michaelis-Menten kinetic curve, and it appeared to have a biphasic kinetics curve (Figure 2-6). At lower cysteine concentration range, from 0 to 500 μM, the data points seem to fit well with the Michaelis-Menten kinetic curve (the hyperbolic phase) and at higher concentration range, from 500 μM to 2 mM, the data points seem to denote the linear nonsaturable phase. The lower cysteine concentration range was replotted with the Michaelis-Menten kinetic fit (Figure 2-7). After fitting the lower cysteine concentration data points to Michaelis-Menten kinetic equation, the apparent kinetic parameters were determined. The k_{cat} was 0.22 ± 0.03 min^{-1} and K_M was found to be 20 ± 14 μM.

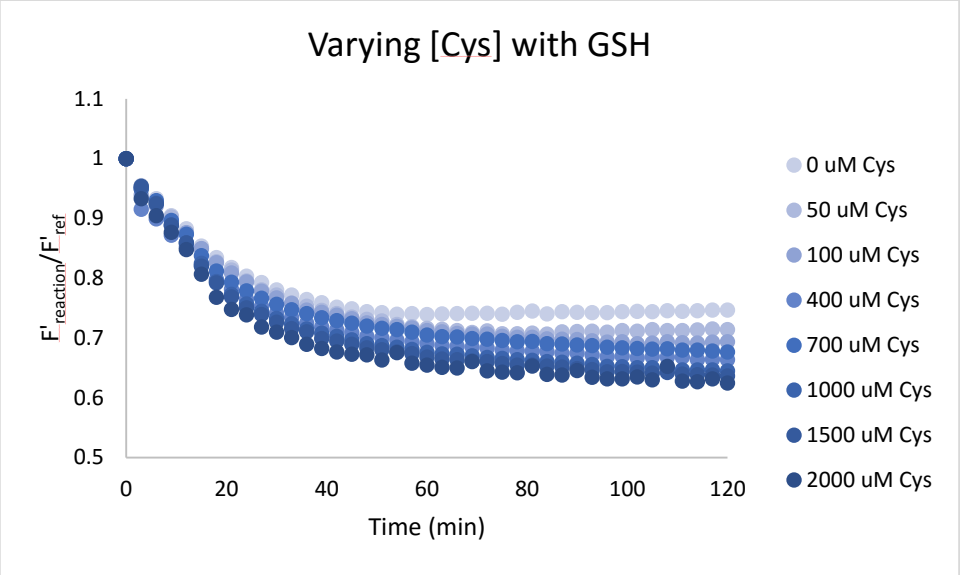

Figure 2-5. [2Fe-2S]-IscU$_{Rho}$ formation with various cysteine concentrations in the presence of glutathione. Reactions contained IscS (0.5 µM), apo-IscU$_{Rho}$ (30 µM), ferrous iron (400 µM), glutathione (10 mM) and different concentrations of cysteine. Fe-S cluster formation was monitored by quenching of IscU$_{Rho}$ as a function of time.

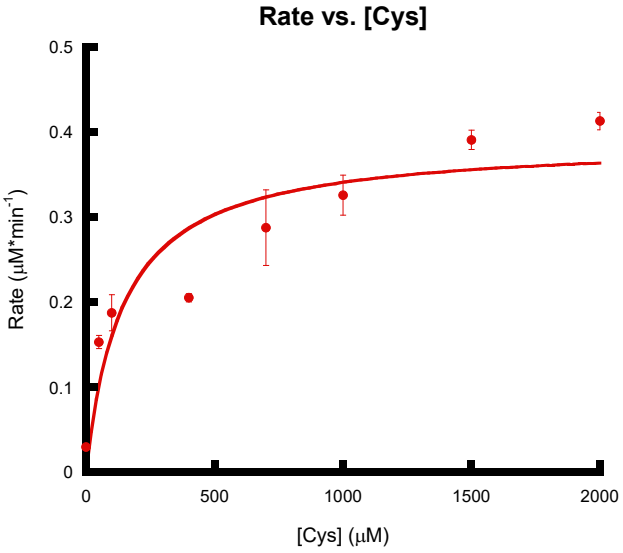

Figure 2-6. The rate of the reaction as a function of cysteine concentration. The plot was generated based on the data from Figure 2-5. The rates for each data points were obtained by multiplying the concentrations of holo-IscU$_{Rho}$ formed at the end of each reactions with rates from the initial linear regions of the quenching data.

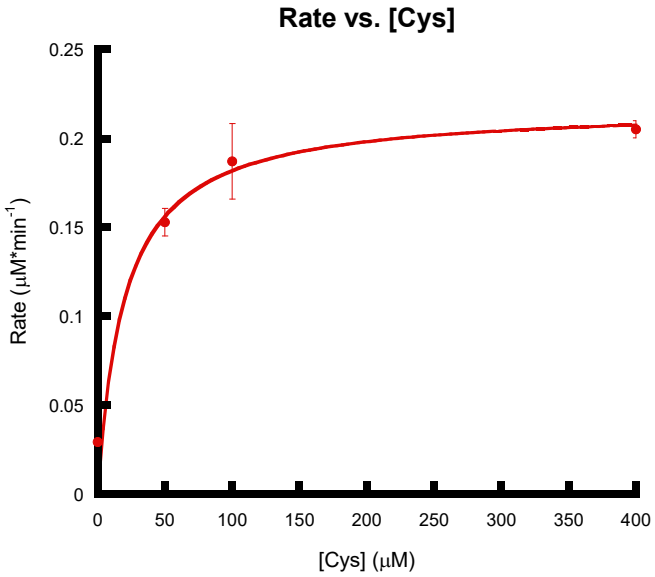

Figure 2-7. The rate of the reaction as a function of lower cysteine concentration. The plot was replotted at the lower cysteine concentration from Figure 2-6. The rates for each data points were obtained by multiplying the concentrations of holo-$IscU_{Rho}$ formed at the end of each reactions with rates from the initial linear regions of the quenching data.

Glutathione Concentration Dependence on the Fe-S Cluster Assembly Reaction.

Next, the concentration of GSH was varied for cluster formation reactions with two different concentrations of cysteine. The experiments were carried out with 100 μM of cysteine and with 1 mM cysteine concentrations. As the concentration of GSH was increased, the rates of [2Fe-2S] cluster formation on $IscU_{Rho}$ increased in a linear fashion for both cysteine concentrations and did not saturate even at 10 mM GSH. The slopes for cluster formation reactions with100 μM and with 1 mM concentrations of cysteine were 0.00082 and 0.031 $\mu M^{-1} \cdot min^{-1}$, respectively, and the linear trend was consistent for both cases.

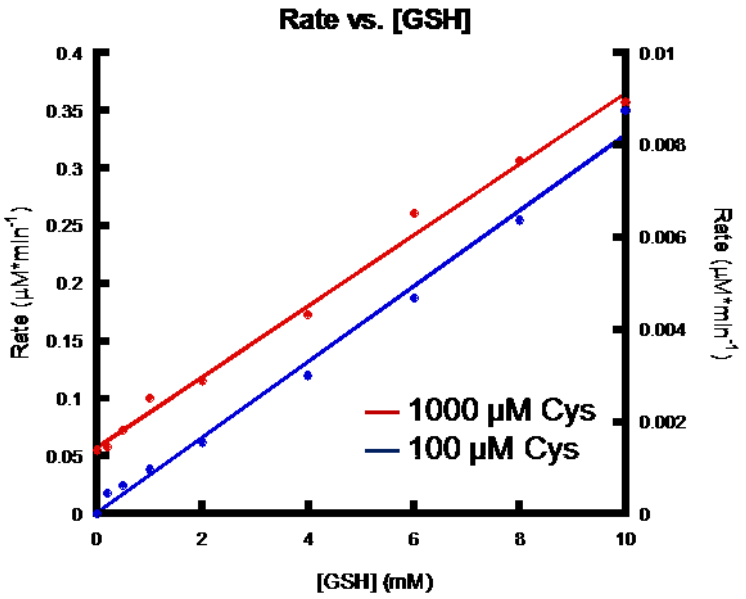

Figure 2-8. The rate of the reaction as a function of glutathion concentration. The plot was generated based on the quenching experiments. The rates for each data points were obtained by multiplying the concentrations of holo-IscU$_{Rho}$ formed at the end of each reaction with rates from the initial linear regions of the quenching data.

IscU Concentration Dependence on the Fe-S Cluster Assembly Reaction. Next, the rate of Fe-S assembly reaction was measured using a concentration of apo-IscU$_{Rho}$ from 15 μM to 100 μM. The quenching rates from each reaction contained different concentrations of apo-IscU$_{Rho}$ were similar to each other (Figure 2-9). At the end of each reaction, all of the reactions quenched to the F'$_{reaction}$/F'$_{reference}$ value of 0.6 which was assumed to be 100% quenching for the apo-IscU$_{Rho}$ concentration that was present in the reaction. Therefore, when the quenching rates were multiplied by the final concentrations of holo-IscU$_{Rho}$, the rate of reaction as a function of apo-IscU$_{Rho}$ concentration displayed a linear relationship (Figure 2-10).

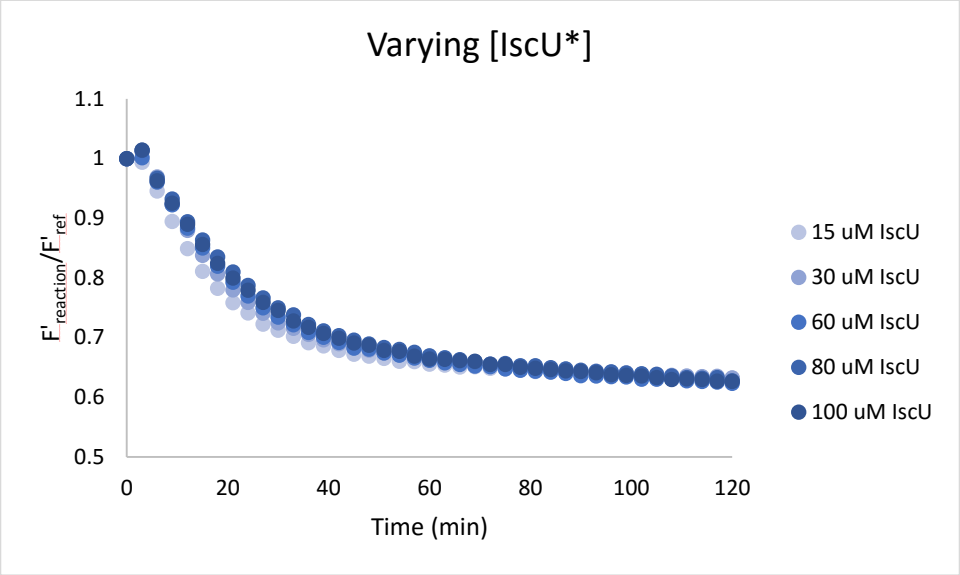

Figure 2-9. [2Fe-2S]-$IscU_{Rho}$ formation with various apo-$IscU_{Rho}$ concentrations in the presence of glutathione. Reactions contained IscS (0.5 μM), ferrous iron (400 μM), L-cysteine (2 mM), glutathione (10 mM) and different concentrations of apo-$IscU_{Rho}$. Fe-S cluster formation was monitored by quenching of $IscU_{Rho}$ as a function of time.

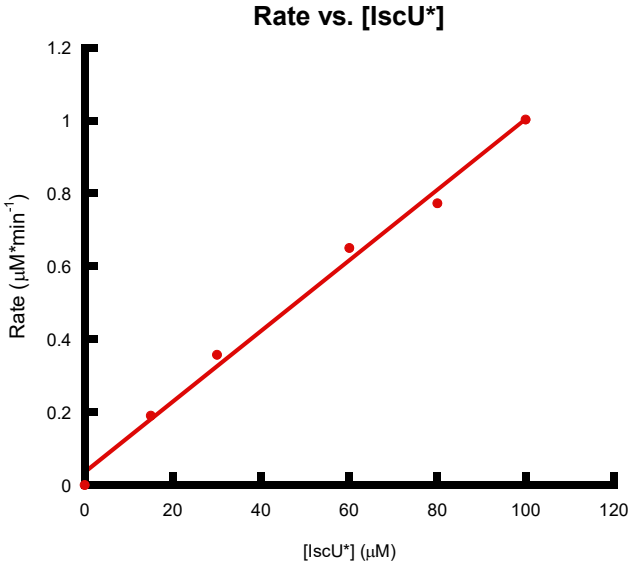

Figure 2-10. The rate of the reaction as a function of apo-$IscU_{Rho}$ concentration. The plot was generated based on the data from Figure 2-9. The rates for each data points were obtained by multiplying the concentrations of holo-$IscU_{Rho}$ formed at the end of each reaction with rates from the initial linear regions of the quenching data.

Cluster Assembly with Different [Fe^{2+}] in Presence of GSH. Finally, the first experiment where the ferrous iron concentration was varied was repeated with various concentrations of apo-$IscU_{Rho}$. From the previous experiment, it was found that 30 μM apo-$IscU_{Rho}$ was not a saturating amount for the cluster assembly reaction. Therefore, 15 μM and 60 μM concentrations of apo-$IscU_{Rho}$ were chosen to carry out the experiment with various ferrous iron concentrations. After plotting the rate of the reaction as a function on iron concentration, each of the experiments with 15, 30, and 60 μM $IscU_{Rho}$ concentrations demonstrated Michaelis-Menten kinetic behaviors. The apparent kinetic parameters are provided in Table 2-1.

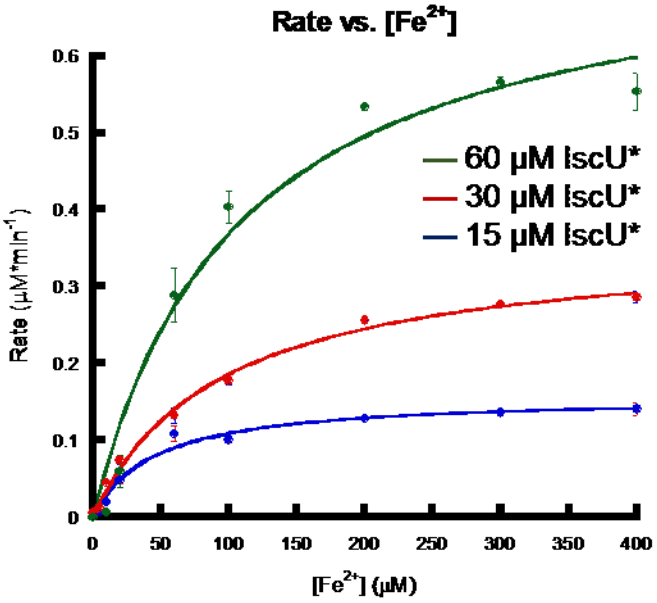

Figure 2-11. The rate of the reaction as a function of ferrous iron concentration. The plot was replotted at the lower cysteine concentration region from Figure 2-6. The rates for each data points were obtained by multiplying the concentrations of holo-$IscU_{Rho}$ formed at the end of each reaction with rates from the initial linear regions of the quenching data.

Table 2-1. Kinetic parameters for [2Fe-2S] cluster formation on IscU with different ferrous iron concentrations.

$[IscU_{Rho}]$ (μM)	k_{cat} (min^{-1})	K_M (μM)
60	0.75 ± 0.07	110 ± 30
30	0.36 ± 0.01	90 ± 10
15	0.16 ± 0.01	44 ± 9

DISCUSSION

Based on the kinetic results, a model for the cluster assembly reaction has been proposed (Figure 2-12). After IscS and IscU interacts to form a complex, holo-IscU can be formed in the presence of ferrous iron, cysteine, and electron source. Once the holo-IscU has formed, the holo-IscU species can be trapped, which can lead to higher fluorescence quenching. Any trapping holo-IscU reaction will show linear nonsaturable trend in the plot of reaction rate versus substrate concentration.

First, the ferrous iron was treated as a substrate and different concentrations of ferrous iron, from 0 to 400 μM, were used for the cluster formation reaction. As the substrate concentration was increased, the rate of reaction displayed a Michaelis-Menten kinetic curve (Figure 2-2). This result indicates the ferrous iron only participates in the enzymatic cluster formation from apo-IscU to holo-IscU and does not interact with holo-IscU once it is formed. 400 μM ferrous iron was used in later experiment as saturating amount of iron concentration.

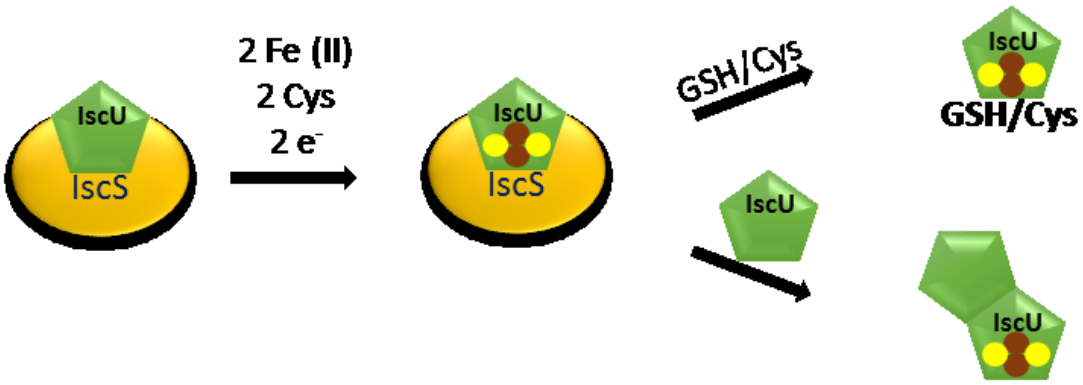

Figure 2-12. Proposed model for the cluster formation reaction in the ISC system.

After observing hyperbolic relationship for cluster formation reaction with varying iron concentration, similar result was expected for varying cysteine concentration since it participates as the sulfur donor in the reaction. However, the rate of reaction as a function of cysteine concentration showed a linear relationship (Figure 2-4). This result hinted that cysteine might have a role in the cluster formation reaction in addition to its function as a source of sulfur. When glutathione (GSH), a physiologically available reducing agent in cells, was introduced in the cluster assembly reaction, cysteine demonstrated different behavior. At lower concentration range of cysteine with the presence of 10 mM GSH, the data followed Michaelis-Menten kinetic curve. At higher concentration range of cysteine with the presence of GSH, the data illustrated nonsaturating linear relationship. These two results indicate cysteine may be playing different role(s) depending on its concentration level in the cluster assembly reaction. When the cluster formation reaction occurs with low concentration of cysteine in the presence of other reducing agent, the primary role of cysteine is a sulfur donor. This enzymatic process fits well with a Michaelis-Menten

kinetic equation (Figure 2-7) and the kinetic parameters are 0.22 ± 0.03 min^{-1} for k_{cat} and 20 ± 14 μM for K_M. Interestingly, the K_M for the bacterial cysteine desulfurase activity was found to be 17 μM [46], which is similar to the cysteine K_M for the Fe-S assembly reaction. On the other hand, cysteine may participate in other steps when it is in high enough concentration. At higher concentration of cysteine, cysteine not only act as a sulfur donor but also act as an electron source and/or as a trapping agent for holo-IscU. Since consistent increase of the rate was reported for the cluster formation reaction with respect to high cysteine concentration, cysteine may contribute to the higher quenching in the reaction by interacting with uncomplexed holo-IscU species and keeping it from reforming a complex with IscS. This would allow IscS to interact with apo-IscU and undergo additional cluster synthesis cycles.

In the cluster assembly reaction with varying GSH concentration, the rate of the reaction was first order with respect to GSH (Figure 2-8). If GSH is only involved in cluster assembly reaction as an electron source, the expected result would be a saturation behavior with the high enough concentration of GSH. Since the result demonstrates nonsaturating linear trend, GSH is acting more than as the electron source. After holo-IscU has been formed, GSH may trap the holo-IscU to form GSH-holo-IscU species, similar to the case with high cysteine concentrations, and thereby contribute to the increased fluorescence quenching.

Similar to cysteine and GSH, varying concentration of apo-IscU in cluster assembly reaction demonstrated the rate to be a first order reaction (Figure 2-10). One of the explanations for this linear behavior in rate would be a dimerization of holo-IscU with

available apo-IscU after the cluster formation (Figure 2-13). These non-enzymatic reactions which may take place after the cluster formation make it hard to monitor just the cluster assembly rate on IscU and contribute to the quenching which complicates the data analysis.

Figure 2-13. Proposed model for the IscU dimerization in the ISC system.

The varying iron concentration experiment was repeated with different concentrations of apo-IscU since we now know that other substrates in that experiment were not at higher or saturating condition. As expected, when the concentrations of apo-IscU were increased, the kinetic parameters were also increased (Table 2-1). If other substrates than ferrous iron were at the saturating condition, the K_M values for different apo-IscU in each reaction should report similar value.

CHAPTER III

CONCLUSIONS

Here we investigated the enzymology of Fe-S cluster assembly in the bacterial ISC system and substrate dependence and/or kinetic parameters were reported. Recently developed fluorescent reporter methodology was utilized to understand the enzyme kinetic of the bacterial Fe-S cluster biosynthetic machinery. Fluorescently labeled IscU was quenched as the cluster was formed on $IscU_{Rho}$. The rate of [2Fe-2S]-$IscU_{Rho}$ formation was determined as a function of each individual substrate with the other substrates at high or saturating conditions.

As the concentration of each of the substrates was varied, the relationship between the rate of the reaction and the substrate concentration was determined. Surprisingly, some of the substrates showed Michaelis-Menten behavior, whereas others showed a linear relationship that did not appear to saturate. Based on our findings, the ferrous iron incorporation only took place in cluster assembly on IscU step. Cysteine acts primarily as a sulfur source for cluster assembly reaction at lower concentration range, while at higher concentration range, it may also act as an electron source and/or as a trapping agent for holo-IscU. Future studies will focus on better elaborating the role of cysteine by investigating the apparent biphasic behavior in Figure 2-6 with additional measurements in the 300 to 800 μM range.

The rate of the reaction was found to be first order with respect to apo-IscU, GSH, and cysteine. These studies reveal that they may play other roles in later step from the formation of holo-IscU. Additionally, evidence has been provided that the quenching

reports not only the formation of complexed holo-IscU but also uncomplexed holo-IscU trapped by other substances.

Importantly, this system can be further developed as a functional assay to evaluate the function of various proteins such as CyaY, IscX, IscA, and Fdx in bacterial Fe-S cluster assembly in the future. Each of these proteins with unknown function can be introduced and the substrate dependency and/or the kinetic parameters can be compared based on our findings. Furthermore, this fluorescent reporter methodology can also be used to study transfer mechanism and better understand the roles of other proteins involved in cluster transfer mechanism.

REFERENCES

1. Lill, R. and U. Muhlenhoff, *Iron-sulfur protein biogenesis in eukaryotes: components and mechanisms.* Annu Rev Cell Dev Biol, 2006. **22**: p. 457-86.
2. Huber, C. and G. Wachtershauser, *Peptides by activation of amino acids with CO on (Ni,Fe)S surfaces: implications for the origin of life.* Science, 1998. **281**(5377): p. 670-2.
3. Fontecave, M., *Iron-sulfur clusters: ever-expanding roles.* Nat Chem Biol, 2006. **2**(4): p. 171-4.
4. Beinert, H., *Iron-sulfur proteins: ancient structures, still full of surprises.* J Biol Inorg Chem, 2000. **5**(1): p. 2-15.
5. Bak, D.W. and S.J. Elliott, *Alternative FeS cluster ligands: tuning redox potentials and chemistry.* Curr Opin Chem Biol, 2014. **19**: p. 50-8.
6. Johnson, D.C., et al., *Structure, function, and formation of biological iron-sulfur clusters.* Annu Rev Biochem, 2005. **74**: p. 247-81.
7. Lill, R., *Function and biogenesis of iron-sulphur proteins.* Nature, 2009. **460**(7257): p. 831-8.
8. Rouault, T.A., *Biogenesis of iron-sulfur clusters in mammalian cells: new insights and relevance to human disease.* Dis Model Mech, 2012. **5**(2): p. 155-64.
9. Brzoska, K., S. Meczynska, and M. Kruszewski, *Iron-sulfur cluster proteins: electron transfer and beyond.* Acta Biochim Pol, 2006. **53**(4): p. 685-91.

10. Bandyopadhyay, S., K. Chandramouli, and M.K. Johnson, *Iron-sulfur cluster biosynthesis.* Biochem Soc Trans, 2008. **36**(Pt 6): p. 1112-9.

11. Henderson, R.A., *Mechanistic studies on synthetic Fe-S-based clusters and their relevance to the action of nitrogenases.* Chem Rev, 2005. **105**(6): p. 2365-437.

12. Holton, B., et al., *Reconstitution of the 2Fe-2S center and g = 1.89 electron paramagnetic resonance signal into overproduced Nostoc sp. PCC 7906 Rieske protein.* Biochemistry, 1996. **35**(48): p. 15485-93.

13. Imlay, J.A. and S. Linn, *DNA damage and oxygen radical toxicity.* Science, 1988. **240**(4857): p. 1302-9.

14. Liochev, S.L., *The role of iron-sulfur clusters in in vivo hydroxyl radical production.* Free Radic Res, 1996. **25**(5): p. 369-84.

15. Wardman, P. and L.P. Candeias, *Fenton chemistry: an introduction.* Radiat Res, 1996. **145**(5): p. 523-31.

16. Nappi, A.J. and E. Vass, *Hydroxyl radical formation resulting from the interaction of nitric oxide and hydrogen peroxide.* Biochim Biophys Acta, 1998. **1380**(1): p. 55-63.

17. Elgrably-Weiss, M., et al., *A Salmonella enterica serovar typhimurium hemA mutant is highly susceptible to oxidative DNA damage.* J Bacteriol, 2002. **184**(14): p. 3774-84.

18. Park, S. and J.A. Imlay, *High levels of intracellular cysteine promote oxidative DNA damage by driving the fenton reaction.* J Bacteriol, 2003. **185**(6): p. 1942-50.

19. Imlay, J.A., *Cellular defenses against superoxide and hydrogen peroxide.* Annu Rev Biochem, 2008. **77**: p. 755-76.

20. Reiffenstein, R.J., W.C. Hulbert, and S.H. Roth, *Toxicology of hydrogen sulfide.* Annu Rev Pharmacol Toxicol, 1992. **32**: p. 109-34.

21. Jacobson, M.R., et al., *Physical and genetic map of the major nif gene cluster from Azotobacter vinelandii.* J Bacteriol, 1989. **171**(2): p. 1017-27.

22. Jacobson, M.R., et al., *Biochemical and genetic analysis of the nifUSVWZM cluster from Azotobacter vinelandii.* Mol Gen Genet, 1989. **219**(1-2): p. 49-57.

23. Hu, Y. and M.W. Ribbe, *A journey into the active center of nitrogenase.* J Biol Inorg Chem, 2014. **19**(6): p. 731-6.

24. Zheng, L., et al., *Assembly of iron-sulfur clusters. Identification of an iscSUA-hscBA-fdx gene cluster from Azotobacter vinelandii.* J Biol Chem, 1998. **273**(21): p. 13264-72.

25. Tokumoto, U., et al., *Interchangeability and distinct properties of bacterial Fe-S cluster assembly systems: functional replacement of the isc and suf operons in Escherichia coli with the nifSU-like operon from Helicobacter pylori.* J Biochem, 2004. **136**(2): p. 199-209.

26. Schwartz, C.J., et al., *IscR, an Fe-S cluster-containing transcription factor, represses expression of Escherichia coli genes encoding Fe-S cluster assembly proteins.* Proc Natl Acad Sci U S A, 2001. **98**(26): p. 14895-900.

27. Giel, J.L., et al., *Regulation of iron-sulphur cluster homeostasis through transcriptional control of the Isc pathway by [2Fe-2S]-IscR in Escherichia coli.* Mol Microbiol, 2013. **87**(3): p. 478-92.

28. Yeo, W.S., et al., *IscR acts as an activator in response to oxidative stress for the suf operon encoding Fe-S assembly proteins.* Mol Microbiol, 2006. **61**(1): p. 206-18.

29. Black, K.A. and P.C. Dos Santos, *Shared-intermediates in the biosynthesis of thio-cofactors: Mechanism and functions of cysteine desulfurases and sulfur acceptors.* Biochim Biophys Acta, 2015. **1853**(6): p. 1470-80.

30. Kato S., et al., *Cys-328 of IscS and Cys-63 of IscU are the sites of disulfide bridge formation in a covalently bound IscS/IscU complex: implications for the mechanism of iron-sulfur cluster assembly.* Proc Natl Acd Sci U S A, 2002. **99**: p. 5948-5952.

31. Wang, W., et al., *In vivo evidence for the iron-binding activity of an iron-sulfur cluster assembly protein IscA in Escherichia coli.* Biochem J, 2010. **432**(3): p. 429-36.

32. Agar, J.N., et al., *IscU as a scaffold for iron-sulfur cluster biosynthesis: sequential assembly of [2Fe-2S] and [4Fe-4S] clusters in IscU.* Biochemistry, 2000. **39**(27): p. 7856-62.

33. Bonomi, F., et al., *Facilitated transfer of IscU-[2Fe2S] clusters by chaperone-mediated ligand exchange.* Biochemistry, 2011. **50**(44): p. 9641-50.

34. Markley, J.L., et al., *Metamorphic protein IscU alternates conformations in the course of its role as the scaffold protein for iron-sulfur cluster biosynthesis and delivery.* FEBS Lett, 2013. **587**(8): p. 1172-9.

35. Kim, J.H., et al., *[2Fe-2S]-ferredoxin binds directly to cysteine desulfurase and supplies an electron for iron-sulfur cluster assembly but is displaced by the scaffold protein or bacterial frataxin.* J Am Chem Soc, 2013. **135**(22): p. 8117-20.

36. Yan, R., et al., *Ferredoxin competes with bacterial frataxin in binding to the desulfurase IscS.* J Biol Chem, 2013. **288**(34): p. 24777-87.

37. Chandramouli, K., et al., *Formation and properties of [4Fe-4S] clusters on the IscU scaffold protein.* Biochemistry, 2007. **46**(23): p. 6804-11.

38. Yan, R., S. Adinolfi, and A. Pastore, *Ferredoxin, in conjunction with NADPH and ferredoxin-NADP reductase, transfers electrons to the IscS/IscU complex to promote iron-sulfur cluster assembly.* Biochim Biophys Acta, 2015. **1854**(9): p. 1113-7.

39. Kim, J.H., et al., *Role of IscX in iron-sulfur cluster biogenesis in Escherichia coli.* J Am Chem Soc, 2014. **136**(22): p. 7933-42.

40. Pastore, C., et al., *YfhJ, a molecular adaptor in iron-sulfur cluster formation or a frataxin-like protein?* Structure, 2006. **14**(5): p. 857-67.

41. Fontecave, M., et al., *Mechanisms of iron-sulfur cluster assembly: the SUF machinery.* J Biol Inorg Chem, 2005. **10**(7): p. 713-21.

42. Shi, R., et al., *Structural basis for Fe-S cluster assembly and tRNA thiolation mediated by IscS protein-protein interactions.* PLoS Biol, 2010. **8**(4): p. e1000354.

43. Vranish, J., et al., *Fluorescent probes for tracking the transfer of iron-sulfur cluster and other metal cofactors in biosynthetic reaction pathways.* J Am Chem Soc, 2015. **137**(1): p. 390-398.

44. Krishnamoorthy, K., et al., *A reagent for the detection of protein thiocarboxylates in the bacterial proteome: lissamine rhodamine B sulfonyl azide.* J Am Chem Soc, 2010. **132**(33): p. 11608-11612.

45. Haugland, R., *Handbook of Fluorescent Probes and Research Chemicals, 6th ed.,* Molecular Probes: Eugene, OR, 1996.

46. Bridwell-Rabb, J., *Effector role reversal during evolution: the case of frataxin in Fe-S cluster biosynthesis.* Biochemistry, 2012. **51**(12): p. 2506-2514.